Reliability Engineering and System Safety 242 (2024) 109712

Contents lists available at ScienceDirect

Reliability Engineering and System Safety

journal homepage: www.elsevier.com/locate/ress

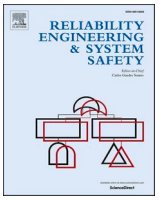

Probabilistic scenario analysis of integrated road-power infrastructures with hybrid fleets of EVs and ICVs

Lida Naseh Moghanlou [a], Francesco Di Maio [a,*], Enrico Zio [a,b]

[a] Department of Energy, Politecnico di Milano, Milan, Italy
[b] Mines Paris, PSL Research University, CRC, Sophia Antipolis, France

ARTICLE INFO

Keywords:
Electric vehicle (EV)
Internal combustion vehicle (ICV)
Road network
Power network
System of systems (SoS)
Transport Reliability (TR)
Service Loss
Probabilistic Scenario Analysis

ABSTRACT

Electric Vehicles (EVs) are key contributors to the reduction of CO2 emissions. However, reliance on EVs must come with the guarantee that the integrated road-power infrastructure is capable of providing adequate mobility serviceability, even in case of disruption due to accidents or disturbances due to traffic jams. In this paper, we propose a probabilistic scenario analysis framework to quantify service losses in terms of delays that vehicles (both EVs and Internal Combustion Vehicles (ICVs)) may incur due to different car accident scenarios. The framework is based on modelling the System of Systems (SoS) comprised by road network, electric power system and vehicles, with graph theory and Finite State Machines (FSMs), respectively, and then embedding the model within a probabilistic scenario analysis, wherein meaningful disruption scenarios are sampled, service losses are measured (specifically as the ratio between the increase in travel time spent along the origin-destination routes on the road network following a disruption, and the corresponding travel time in nominal traffic conditions), and the economic losses and transport reliability of the infrastructure are assessed. To exemplify the application of the framework, we consider a benchmark road-power infrastructure in New York state travelled by a mixed fleet of EVs and ICVs, with different EVs penetration levels and under car accidental scenarios of different magnitudes. By using the insightful graphical representation of the results in terms of traffic volume across different road sections, the framework allows comparing alternative road-power infrastructure designs (e.g., critical roads, optimal gas and charging station locations, power network structure and topology, …) with respect to travel times, economic service losses and transport reliability considering different nominal and disruption scenarios under different EVs penetration levels service.

1. Introduction

THE transportation network is considered one of the most crucial lifelines of modern society. To deal with the reduction of CO_2 emissions, and supported by fast technological development, transportation network is exposed to the uncertain and unknown effects of the increasing penetration by Electric Vehicles (EVs), that makes it strongly dependant on power distribution systems. This calls for a System of Systems (SoS) concept to study the attributes and performance [1–7] for the integrated road-power network [2–9]. In relation to the reliability performance of the integrated road-power network, the concern is that disruptions and disturbances on the transportation network may affect the power distribution system, and vice versa, causing travel time increases and service losses [10]. To analyse these problems, the concept of travel time reliability has been defined [11], as the probability that travel time between a pair of Origin-Destination (O-D) nodes is less than a threshold value, which defines the condition of no delay [10]. Also, any occurring delay can be mapped into a cost to compute the economic losses due to the disruption [12].

Up to now, studies have been focusing on the assessment of the reliability and service losses i.e., the serviceability of conventional road networks (that is, not integrated with power networks in a SoS perspective) and mainly from a topological (i.e., network connectivity) perspective: the economic impact of service losses for integrated road-power networks has not been studied in depth, whereas it is needed to design, build and operate the reliable infrastructures of tomorrow. The challenge is even more relevant when we consider a hybrid fleet of EVs and ICVs running on an integrated road-power network originally designed solely for ICVs. Indeed, the current integrated road-power infrastructures require a limited amount of electricity to be supplied, mainly devoted to auxiliary services such as street lighting [13],

* Corresponding author.
E-mail address: francesco.dimaio@polimi.it (F. Di Maio).

https://doi.org/10.1016/j.ress.2023.109712
Received 13 January 2023; Received in revised form 20 September 2023; Accepted 3 October 2023
Available online 7 October 2023

Notation

G	Road network graph
$\overline{\overline{C}}$	Matrix of the capacity of the edges of G
$\mathscr{V}$	Set of nodes of G
i	Node index of G
j	Node index of G
H	Total number of nodes of G
$\overline{\overline{A}}$	Adjacency matrix of G
$a^{i,j}$	Number of lanes connecting edge i,j
$c^{i,j}$	Maximum number of vehicles which can drive along the edge i,j
$\overline{\overline{\varepsilon}}$	Matrix of edges of G
$\varepsilon^{i,j}$	Edge length connecting the i th and the j-th nodes of G
R	Total number of roads of G
μ	FSM model
S	Set of states of μ
S_m	m-th state of μ
M	Total number of states of μ
f	Transition function of μ
$\overline{\theta}$	Set of context parameters of f
θ_l	l-th context parameter of f
L	Total number of context parameters of f
EV_r	r-th EV
N_{EVs}	Total number of EVs
ICV_p	p-th ICV
N_{ICVs}	Total number of ICVs
t	Time
T	Time interval
$N_{\mathcal{R}}^{i,j}(t)$	Number of vehicles in the edge i,j of road section $\mathcal{R}$ at time t
$N_{CS_x}(t)$	Number of vehicles at the charging station CS_x at time t
$N_{GS_\xi}(t)$	Number of vehicles at the gas station GS_ξ at time t
$CH_x(t)$	Power demand of charging station x at time t
$ch_r(t)$	Power demand of EV_r at time t
E^{tot}	Power demand of the integrated road-power infrastructure
$SoC_r(t)$	SoC of EV_r at time t
$SoC_{critical}$	Critical SoC for an EV
$FL_p(t)$	FL of ICV$_p$ at time t
$FL_{critical}$	Critical FL for an ICV
$FL_{critical-c}$	Critical FL for a commercial ICV
P_d	Driving power of EVs
P_q	Queuing for traffic power of EVs
P	Charging power of EVs
F_p^{dr}	Driving fuel consumption rate for ICV_p
F_p^{id}	Idling fuel consumption rate for ICV_p
B_r	Battery capacity of EV_r
$Tank_p$	Tank capacity of non-commercial ICVs
$Tank_{p-c}$	Tank capacity of commercial ICVs
$t_{r,in}$	Entrance time of EV_r
$t_{p,in}$	Entrance time of ICV_p
t_r^{ch}	Charging time
Tr_{EV_r}	Travel time of EV_r
Tr_{ICV_p}	Travel time of ICV_p
U	Constant speed
q_v	Refilling rate of non-commercial ICVs
q_{v-c}	Refilling rate of commercial ICVs
α	EV penetration level
φ	Turning parameter
Q	Power network graph
$\mathcal{R}$	Set of road sections
R	R-th road section
CS	Set of charging stations
CS_x	Charging station fed by the x-th bus
GS	Set of gas stations
GS_ξ	ξ-th gas station
$\mathcal{E}$	Total number of gas stations
W	Set of buses of Q
w_x	x-th bus
X	Total number of buses of Q
Z	Set of branches of Q
Γ	Constant value for economic service losses
λ	Economic service loss threshold
ρ	Severity of car accident on the road-power infrastructure
$SL_{EV_r \text{ or } ICV_p}(\rho)$	Services losses of EV_r or ICV_p
$ESL_{EV_r \text{ or } ICV_p}(\Gamma,\rho)$	Economic service losses of EV_r or ICV_p

Acronyms

AADT	Annual Average Daily Traffic
CTM	Cell Transmission Model
DFDM	Deterministic Fluid Dynamic Model
DTA	Dynamic Traffic Assignment
ELR	Energy Loss Rate
EV	Electric Vehicle
FL	Fuel Level
FSM	Finite State Machine
HTAF	Hourly Temporal Allocation Factor
HTD	Hourly Traffic Demand
ICV	Internal Combustion Vehicle
LoC	Level of Congestion
LP	Linear Program
NVD	Nodal Voltage Deviation
O	Origin
D	Destination
O-D	Origin-Destination
PDS	Power Distribution System
SoC	State of Charge
STM	Spatial-Temporal Model
SUEM	Static User Equilibrium Model
TR	Transport Reliability
UTAM	Unconstrained Traffic Assignment Model

whereas with the increasing penetration of EVs, power networks are challenged, particularly because EVs charging loads vary over time and spatially due to the EVs mobility and relatively long charging time [14]: this leads to changing from the typical constant (in time and in space) power load profile to a dynamic, distributed load profile. In this scenario, the concern is that widespread use of EVs can expose the current road-power infrastructure to disruptive events (with consequent service losses), if instances such as congestion of charging stations and of transmission lines are not properly considered and dealt with [15,16].

Considering the aforementioned concerns, the research gaps addressed in this work are filled by developing:

- a SoS approach to assess the mutual effects of events occurring on the road network and power grid,
- a framework that accounts for the evaluation of dynamic distributed power profiles,
- a stochastic approach for the evaluation of road-power network disruption scenarios,
- a metric to measure the economic losses and transport reliability of integrated road-power networks, in presence of hybrid fleet of EVs and ICVs.

To do this, we propose a novel probabilistic scenario analysis

framework that is based on an integrated model that accounts for the interconnections and interactions within the road-power SoS [17–19], and is used to quantify a set of performance metrics [20] under nominal condition and disruption scenarios [21,22].

The SoS model consists of a set of dynamically interacting models, namely, those of the road and electric power networks, and the vehicles fleet. We use graph theory to model the topological structure of the road network [23–25]. The electric power network topology is also modelled using graph theory and its response evaluated with a single-phase AC power flow, a widely accepted high-quality approximation of the steady-state behaviour of a real-world power flow [26,16]. Vehicles fleet motion is modelled by Finite State Machines (FSMs), a promising approach amongst the so called single-vehicle models [27,24] that are aimed to modelling each vehicle separately, and, then, the interactions with the other vehicles. Despite the larger computational cost, single-vehicle methods are more effective in capturing changes in traffic volume during accidents, compared to flow-vehicle methods [16]: the flow-vehicle methods, average the vehicles motion, somehow overlooking traffic congestions and travel time delay that may result in extra energy consumptions. Moreover, FSM, by capturing the real spatial-temporal features of EVs charging demands and the effects that traffic congestions may bring beyond the road-power system domain, are suitable for the reliability assessment of road-power networks. To name few examples of single-vehicles methods, [28] presented an O-D model for EV motion and combined it with Monte Carlo simulation for estimating the EV charging load within a Spatial-Temporal Model (STM) framework; [15] analysed how EVs mobility impacts on the characteristics of a power network (in terms of Level of Congestion (LoC), Nodal Voltage Deviation (NVD) and Energy Loss Rate (ELR)); [29] proposed a rectangular coordinate road model for simulating EV motion that, in combination with a bidirectional charging control strategy, is used to assess the reliability of an integrated transportation-power infrastructure; [24] utilized FSM to model EV motion on transportation networks to optimally schedule the charging of long-range batteries.

As said, differently from single-vehicle models, flow-vehicle models describe vehicles motion based on an "integral" perspective [30,31]. These can be classified in Deterministic Fluid Dynamic Models (DFDMs), Static User Equilibrium Models (SUEMs) and Cell Transmission Models (CTMs). [32] used a DFDM based on the conservation equation of traffic flow for assessing charging demand in charging stations; [33] used a SUEM for the optimal design of charging station location and capacities; [34] proposed an Unconstrained Traffic Assignment Model (UTAM), i.e., a SUEM, to simulate realistic traffic flows in transportation networks; [35] proposed a SUEM that considers also travellers recharging decisions, and captures the impact of recharging time and anxiety of drivers on travel time and route selection; [36] developed a SUEM for modelling congested regional transportation networks where recharging or battery-swapping stations for EVs are scarce; [37] considered a CTM for modelling the interactions between a time-varying urban transportation system and a power distribution system; [16] modelled a highway traffic flow by a CTM, to evaluate the spatial-temporal EV charging loads in different areas of an electrified transportation system.

All the above-mentioned research studies have been focused on modelling the EVs motion on actual road networks, while not considering the still massive presence of ICVs that still play a crucial role, especially in terms of traffic congestion. To fill this gap, in this paper we build FSMs to model both EVs and ICVs which as a single-vehicle method is practical to study the interaction of them on a typical transportation network.

We realistically model the drivers attitudes in selecting alternative routes along the O-D travel in case of car accidents and the consequent traffic congestions that arise. In doing so, we account for the charging and refilling time that, in turn, depends also on the EVs battery capacity and ICVs tank capacity, and the charge and fuel consumption rates.

The developed model is embedded within a probabilistic scenario analysis framework to quantify, at SoS level, the service losses, the associated economic losses and the overall transport reliability (i.e., the serviceability), in relation to the delays that vehicles (both EVs and ICVs) incur due to different car accidental scenarios.

Since the delay in travel time is the triggering event of economic service losses, it is here used as an important metric for quantifying the reliability and service losses with a probabilistic perspective. A realistic case study is considered, concerning the travel of both EVs and ICVs on a road network in New York State. Different levels of EVs penetration are considered and FSM is shown to provide a powerful modelling framework that can include various characteristics of the SoS dynamics, such as drivers attitudes, traffic congestion, and disruptive effects induced by traffic incidents on the EVs and ICVs motion [20]. For the performance of the integrated road-power infrastructure, with a hybrid fleet of EVs and ICVs under different disruption scenarios, in line with [38], we quantify the service losses related to delays that the vehicles may incur in the different accidental scenarios. For the quantification, we use the ratio between the increase in travel time on the O-D routes of the road network due to a disruption and the corresponding expected time in nominal travel conditions. Then, the economic losses associated to the delays are evaluated in line with [12] and finally, the Transport Reliability (TR) is estimated [10].

The remainder of the paper is as follows: Section 2 provides a description of the modelling approaches adopted for the integrated road-power infrastructure, the EVs and ICVs, and the quantification of the service losses and TR; Section 3 presents the application of the proposed modelling framework to the selected case study; Section 4 shows the results, and in Section 5 some conclusions are drawn.

2. Methodology

In this Section, we describe the framework for modelling the SoS comprised by road network, electric power system and vehicles. Graph theory and FSMs are used, respectively, and probabilistic scenario analysis is performed by sampling meaningful disruption scenarios, and assessing the associated economic losses and overall transport reliability. The overall framework is sketched in Fig. 1.

2.1. The integrated road-power infrastructure

The integrated road-power infrastructure is composed by a set of interconnected and interdependent subsystems: the road network, the vehicles and the electric power system, whose detailed modelling solutions adopted are described in Sections 2.1.1, 2.1.2 and 2.1.5, respectively.

2.1.1. The road network

The road network is modelled as a connected graph $G(\mathscr{V};\overline{\overline{\varepsilon}};\overline{\overline{A}};\overline{\overline{C}})$ [24], where $\mathscr{V} = \{1, 2, \ldots, i, \ldots, H\}$ is a non-empty set of H nodes, $\overline{\overline{\varepsilon}}$ is a matrix whose element ε^{ij} is the edge (road) length connecting the i-th and the j-th nodes ($i = 1, \ldots, H$ and $j = 1, \ldots, H$, with $i \neq j$), $\overline{\overline{A}}$ is a weighted adjacency matrix, whose element a^{ij} is the number of lanes connecting the i-th and the j-th nodes, and $\overline{\overline{C}}$ is the capacity matrix, whose element c^{ij} is the maximum number of vehicles which can drive between the i-th and the j-th nodes at the same time. We consider that the road network is composed of a set of R road sections $\mathscr{R} = (1, 2, \ldots, R, \ldots, R)$, a set of X charging stations $CS = (CS_1, CS_2, \ldots, CS_x, \ldots, CS_X)$ and a set of Σ gas stations $GS = (GS_1, GS_2, \ldots, GS_\xi, \ldots, GS_\Sigma)$..

2.1.2. Finite state machine for modelling vehicle motion

Vehicles motion is modelled by FSM, assuming that it is a process of transition through different states, defined by a set of rules [39,40]. In practice, a FSM (an example is sketched in Fig. 2) is a model $\mu(S,f)$ where S is a finite set of M states $S=\{S_0, S_1, \ldots, S_m, \ldots, S_M\}$, with S_0 being the initial state (start-up), S_M the final state (shut-down) and $f(S_m, i, \overline{\theta})$

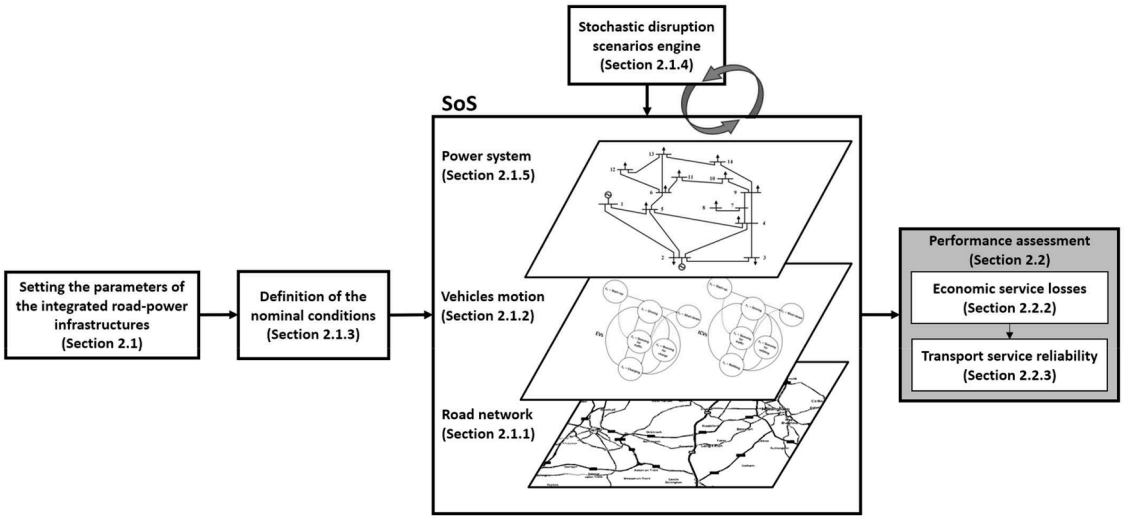

Fig. 1. The probabilistic framework for the scenario analysis.

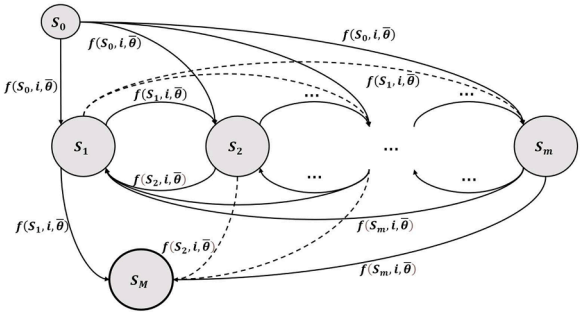

Fig. 2. Sketch of a generic FSM with M States.

a transition rule that depends on the vehicle m-th state S_m, the i-th node the vehicle is passing through and the values taken by a set of L context parameters $\overline{\theta}(\theta_1, \theta_2, \ldots, \theta_l, \ldots, \theta_L)$, such as road traffic congestion, EV current State of Charge (SoC), Fuel Level (FL), drivers road selection attitude (i.e. φ turning), etc. [27,41,42]. In the Appendix A, the FSM developed to model EVs and ICVs are described. In Fig. 3, the resulting FSM structure is shown.

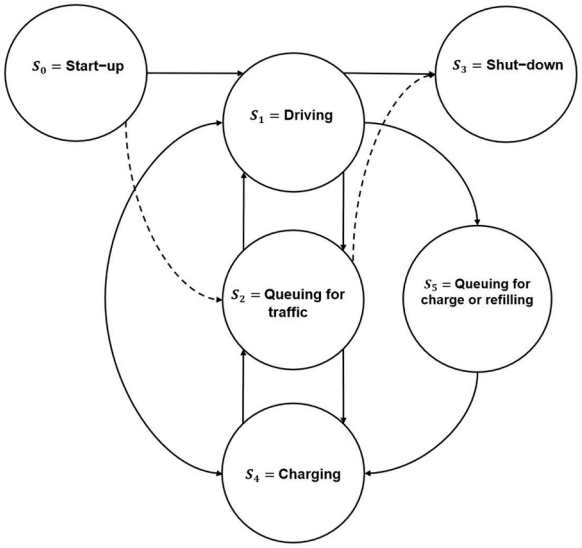

Fig. 3. FSM for an EV or ICV.

To describe the vehicles flow, at each time t we collect the number of EVs and ICVs, $N_R^{i,j}(t)$, passing through (or stopping at) each node i, edge i,j, charging station CS_x, and gas station GS_{ξ}, along with the following information (summarized in Table 1):

- ID of the p-th ICV_p, and the r-th EV_r
- Entrance time of ICVs and EVs into the road-power network, $t_{p,in}$ and $t_{r,in}$, respectively
- EVs entrance SoC, $SoC_r(t_{r,in})$
- ICVs entrance FL, $FL_p(t_{p,in})$
- Drivers charging attitude, $ch_r(t)$
- Refilling FL, $Tank_p$ *or* $Tank_{p-c}$
- SoC profile, $SoC_r(t)$
- FL profile, $FL_p(t)$
- Travel time for each vehicle, Tr_{EV_r}, Tr_{ICV_p}.

This allows collecting trajectories (i.e., time series) of travelled nodes and states (S_0, S_1, S_2, S_3, S_4, S_5) for each vehicle EV_r and ICV_p, traffic volume $N_R^{i,j}(t)$, $SoC_r(t)$, $FL_p(t)$, $N_{CS_x}(t)$ or $N_{GS_{\xi}}(t)$, $CH_x(t)$ for each edge i,j, charging station CS_x and gas station GS_{ξ}. The availability of such multi-dimensional time series is the main benefit of the modelling framework proposed with respect to flow-vehicles models that lump all this information in integral flow-related measures that lack of details with respect to the state of the vehicles running on the road system [20].

Table 1
List of available information of the FSM for vehicles.

EVs	ICVs	Road-power network
ID (EV_r)	ID (ICV_p)	Traffic volume $N_R^{i,j}(t)$ in edge i,j of road R at time t
Entrance time, $t_{r,in}$	Entrance time, $t_{p,in}$	Number of EVs, in charging station CS_x at time t, $N_{CS_x}(t)$
Entrance SoC, $SoC_r(t_{r,in})$	Entrance FL, $FL_p(t_{p,in})$	Power demand in charging station, $CH_x(t)$
Drivers charging attitude, $ch_r(t)$	FL profile, $FL_p(t)$	Power demand of entire system, $E^{tot}(t)$
SoC profile, $SoC_r(t)$	Time series of travelled nodes	Number of ICVs in gas station G_o at time t, $N_{G_o}(t)$,
Time series of travelled nodes	Time series of states, (S_0, S_1, S_2, S_3, S_4, S_5)	Fuel demand in gas station
Time series of states, (S_0, S_1, S_2, S_3, S_4, S_5)	Travel time, Tr_{ICV_p}	Fuel demand of entire system
Travel time, Tr_{EV_r}		

2.1.3. Modelling travel under nominal conditions

For nominal conditions, i.e., no car accidents or disruption and $N_R^{i+1,j+1}(t) < C^{i+1,j+1}$, daily traffic patterns of the vehicles motion are modelled considering the drivers road selection attitude: each vehicle EV_r or ICV_p starts the trip at the Origin (O) with $SoC_r(t_{r,in})$ or $FL_p(t_{p,in})$; during the travel, at each time interval T, it consumes P_d or F_p^{dr}; when it passes by a charging station CS_x or gas station GS_ξ, recharge or refill is performed in case the $SoC_r(t)$ or $FL_p(t)$ equals the critical amount $SoC_{critical}$ or $FL_{critical}$ or $FL_{critical-c}$ that would not allow the vehicle to reach to the next charging station CS_{x+1} or gas station $GS_{\xi+1}$, or the vehicle travels to the node where an intersection is reached and where, depending on the driver turning rate parameter φ (here considered equal to 0.5), one of the other roads is selected; the travelling motion cycle continues until Destination (D) is reached.

At the charging station CS_x, in case of availability of the charger, an EV_r is charged depending on the driver charging attitude $ch_r(t)$; and then, EV_r leaves the charging station with $SoC_r(t)$; otherwise, EV_r waits for a charger to become available.

At the gas station GS_ξ, in case of availability of a fuel pump, an ICV_p is refilled depending on the $Tank_p$ or $Tank_{p-c}$ and, then, it leaves the gas station; otherwise, it waits for a fuel pump to become available.

2.1.4. Modelling disruption scenarios

Disruption is modelled as traffic congestion that randomly occurs at a node of the road network for a duration ρ (hereafter also called severity), during which vehicles are temporarily trapped in a "queuing for traffic" state: when vehicle EV_r or ICV_p is stuck in the traffic jam, it consumes P_q or F_p^{id} or F_{p-c}^{id} until it can move forward to the following road network node; when the vehicle reaches an intersection, for the "next road selection" the rule adopted is that the EV_r or ICV_p always takes the less crowded path, resulting in a shorter or longer path than the path travelled in the nominal conditions scenario. The charging or refilling logic is the same adopted for the nominal conditions travel.

2.1.5. Power flow for modelling the power network

The power network functioning is modelled by a single-phase AC power flow [16] that solves the dispatchment problem for an undirected graph Q (W, Z) comprised of a set of buses $W=\{w_1, w_2 \ldots, w_x, \ldots, w_X\}$, each one feeding a charging station CS_x and a set of branches Z. Power demand $CH_x(t)$ at the x-th charging station CS_x at time t, is calculated from Eq. (1):

$$CH_x(t) = \sum_{r=k} ch_r\ (t) \tag{1}$$

where $ch_r(t)$ is the power demand of the r-th EV being charged at time t, and k is the total number of EVs charged in CS_x.

The power demand $E^{tot}(t)$ of the entire system at time t is calculated as:

$$E^{tot}(t) = \sum_{tot=1}^{X} CH_x(t) \tag{2}$$

2.2. Performance metrics

2.2.1. Service losses

Travel time is one of the most important trip characteristics for individual drivers. It has long been considered as the major influencing factor of transportation system performance [10,38]. Here, we use travel time to reflect the transportation network service level and estimate system services losses. For a specific car accident of severity ρ on the road-power infrastructure, Eq. (3) estimates the service losses $SL_{EV_r \text{ or } ICV_p}(\rho)$ for each EV_r or ICV_p:

$$SL_{EV_r \text{ or } ICV_p}(\rho) = \frac{\Delta Tr_{EV_r \text{ or } ICV_p}(\rho)}{Tr_{EV_r \text{ or } ICV_p}(0)} \tag{3}$$

where

$$\Delta Tr_{EV_r \text{ or } ICV_p}(\rho) = Tr_{EV_r \text{ or } ICV_p}(\rho) - Tr_{EV_r \text{ or } ICV_p}(0) \tag{4}$$

and $Tr_{EV_r \text{ or } ICV_p}(\rho)$ and $Tr_{EV_r \text{ or } ICV_p}(0)$ are the travel times of each EV_r or ICV_p, under disruption and nominal conditions, respectively.

2.2.2. Economic service losses

Travel time is related with power or fuel consumption and, therefore, power or fuel cost of individual vehicles [43]. Economic service losses are, then, dependant on the service losses $SL_{EV_r \text{or } ICV_p}(\rho)$, considering (without loss of generality) a linear relationship; then, they are, in turn, dependant on the travel time. Economic service losses $ESL_{EV_r \text{ or } ICV_p}(\Gamma, \rho)$ caused by a disruption of severity ρ, for a specific EV_r or ICV_p are defined as in Eq. (5) [12]:

$$ESL_{EV_r \text{ or } ICV_p}(\Gamma, \rho) = \Gamma SL_{EV_r \text{ or } ICV_p}(\rho) \tag{5}$$

where Γ is a constant value that is representative of the cost that service losses impose to the system.

2.2.3. Transport reliability

Transport Reliability (TR) provides a useful measure for the service performance of the integrated road-power network, and constitutes useful information for the travelers (especially EV drivers), regarding the effects that route selection and charging timing may have on the travel time. TR is traditionally defined as the probability that vehicles successfully complete their trips within a desired time interval [9], and is here related to the economic service losses, $ESL_{EV_r \text{ or } ICV_p}(\Gamma, \rho)$: then, it can be interpreted as the probability that the vehicles $ESL_{EV_r \text{ or } ICV_p}(\Gamma, \rho)$ are less than a loss threshold (λ), that is representative of the maximum acceptable economic service losses, as defined in Eq. (6):

$$TR = P\left(ESL_{EV_r \text{ or } ICV_p}(\Gamma, \rho) \leq \lambda\right) \tag{6}$$

3. Case study

The case study used in [16] is here adapted to the objective of the current study. The transportation network is considered a comprehensive sample of a part of the national highway system of New York State (Fig. 4(a)), whose topological structure consists of $R = 11$ road sections (Fig. 4(b)). As described in Section 2.1, the physical network is mapped into a homogeneous graph G with $H = 224$ nodes (Fig. 4(c)) connected with edges ε^{ij}, all of the same length equal to 1.0833 *mi*. Solid lines denote a direct connection between two nodes, whereas dashed lines represent that some intermediate nodes are omitted. Vehicles can enter the road network either from node 1 or from node 22, and exit either from node 203 or from node 224.

The hourly traffic pattern related to the selected network is extracted from the Hourly Traffic Demand (HTD) curve [16] widely used as benchmark traffic assignment model [16,20,44,45]:

$$HTD(t) = AADT \times HTAF(t) \tag{7}$$

where $AADT$ is the Annual Average Daily Traffic $(N_{ICVs} + N_{EVs}) = 225{,}780$ vehicles [16] and $HTAF$ is the Hourly Temporal Allocation Factor that accounts for the day of the week and the month of the year considered and is shown in Fig. 5 for the roads US11 and NY190, and the cumulative value of both [44,45].

To assess the effect of the penetration of EVs in the transportation network on the service losses and TR of the SoS, different EV penetration levels (α) are considered. Table 2 summarizes the modelling parameters assumed for the road network.

When in "driving" state, both ICVs and EVs are modelled to run at a

(a) A part of the national highway system of New York State

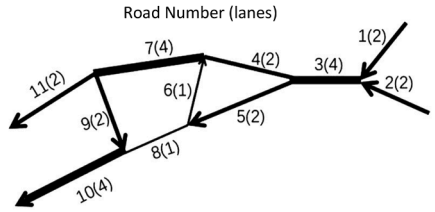

(b) The topological structure of the highway system considered

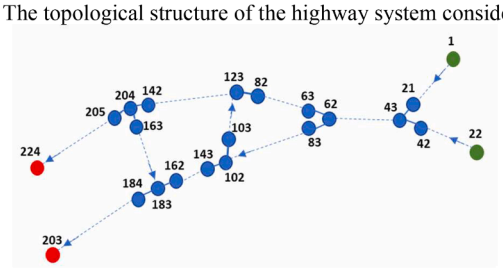

(c) Graph of the network studied

Fig. 4. The test road network [16].

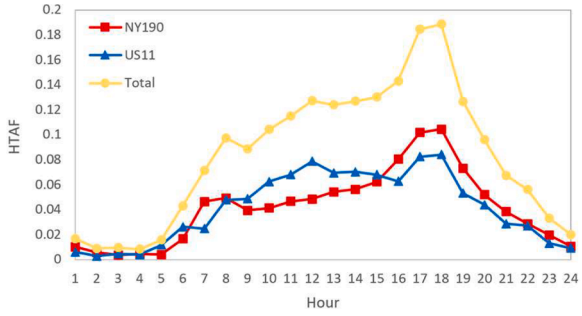

Fig. 5. *HTAF* of the roads,.

Table 2
Parameters of the network.

Parameters		Symbols	Values
Road	Number of nodes	H	224
	Edge length (mi)	$\varepsilon^{i,j}$	1.0833
	Maximum number of vehicles per lane in the edge i,j	$c^{i,j}$	200
	Turning parameter	φ	0.5
Travel time interval (min)		T	1

constant speed of $U = 65$ mph.

Each EV is characterized by:

- Battery capacity B_r: a random B_r following a truncated Normal distribution $\mathbb{N}(24,10)$, in the range $min = 10$ and $max = 90$ (kWh) [46,47].
- State of charge $SoC_r(t_{r,in})$: a random SoC uniformly distributed within the range of battery capacity B_r.
- $SoC_{critical}$: the minimum SoC is insufficient to reach the next charging station CS_{x+1}.
- Power demand $ch_r(t)$: vehicles charge 80 % of their battery in the charging stations in order to recharge fast [46]; therefore, $ch_r(t)$ follows a truncated Normal distribution $\mathbb{N}(20,10)$, in the range $min = 10$ and $max = 90$ (kWh), corresponding to B_r distribution.
- Charging time t_r^{ch}: we assume a linear relationship between the charging time t_r^{ch} and the energy stored in the battery $ch_r(t)$, then, t_r^{ch} can be estimated according to Eq. (8), assuming that the drivers charging attitude $ch_r(t)$ and the charging power P of EVs are known [48]:

$$t_r^{ch} = \frac{ch_r(t)}{P} \tag{8}$$

ICVs are categorized in commercial and non-commercial [49], and each ICV is characterized by:

- Tank capacity of non-commercial vehicles $Tank_p$: a random $Tank_p$ capacity following a truncated Normal distribution $\mathbb{N}(60,5)$, in the range $min = 40$ and $max = 70$ (L) as shown in Fig. 5 [50].
- Tank capacity of commercial vehicles $Tank_{p-c}$: a random $Tank_{p-c}$ capacity following a truncated normal kernel distribution with two picks 350, 950, Bandwidth 50, and in the range $min = 70$ and $max = 1250$ (L), as shown in Fig. 7 [51,52,53].
- F_p^{dr}: driving fuel consumption rate F_p^{dr} corresponding to the randomly selected tank capacity $Tank_p$ in Fig. 6.
- F_{p-c}^{dr}: driving fuel consumption rate F_{p-c}^{dr} corresponding to the randomly selected tank capacity $Tank_{p-c}$ in Fig. 7.
- F_p^{id}: idling fuel consumption rate F_p^{id} corresponding to the randomly selected tank capacity $Tank_p$ in Fig. 6.
- F_{p-c}^{id}: idling fuel consumption rate F_{p-c}^{id} corresponding to the randomly selected tank capacity $Tank_{p-c}$ in Fig. 7.
- $FL_p(t_{p,in})$: a random FL uniformly distributed within the range of tank capacity $Tank_p$ or $Tank_{p-c}$.
- Refilling time t_p^{refill}: assuming a linear relationship between t_p^{refill} and $Tank_p$ or $Tank_{p-c}$, t_p^{refill} can be estimated according to Eq. (9) considering the refilling rate of gas pump q_v or q_{v-c}:

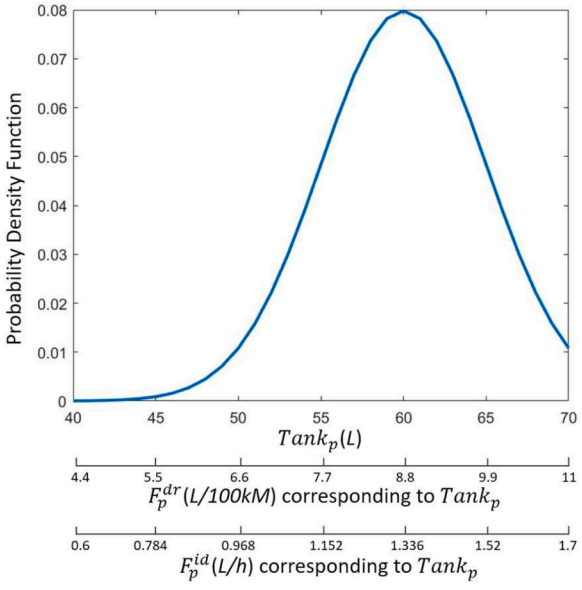

Fig. 6. Tank capacity of non-commercial ICVs.

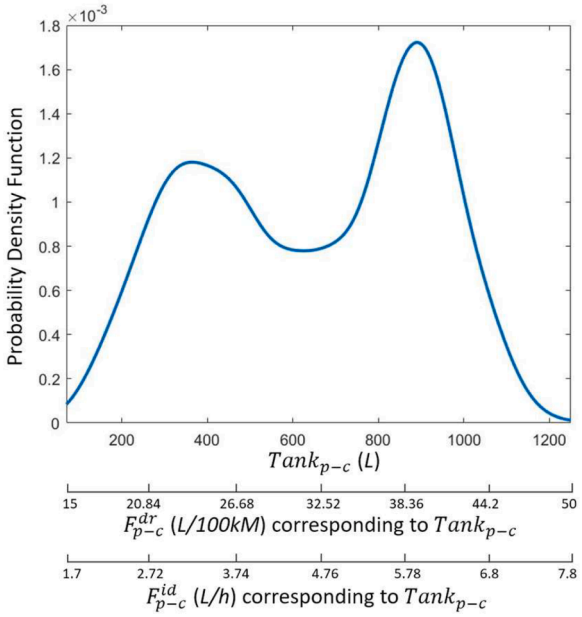

Fig. 7. Tank capacity of commercial ICVs.

$$t_p^{refill} = \frac{Tank_p}{q_v} \text{ or } t_p^{refill} = \frac{Tank_{p-c}}{q_{v-c}} \quad (9)$$

- $FL_{critical}$ or $FL_{critical-c}$: the minimum FL in ICV_p tank that is not sufficient to reach to the next gas station $GS_{\xi+1}$, based on its F_p^{dr} or F_{p-c}^{id}.

Table 3 List of the parameters assumed to model ICVs and EVs.

For the power distribution infrastructure, it is assumed that a charging station (of unlimited maximum capacity) is located in the middle of each road section ($X = 11$) providing the required power demand (Eq. (1)).

4. Results

In this Section, without loss of generality, two disruption scenarios with severity ρ of 1 hour, a negligible disruption, and 2 hours, a severe disruption, are presented for two different road sections, i.e., road 2 (with two lanes and expected not to be too much exposed to traffic jam) and road 3 (with four lanes and more exposed to traffic jam, since all the vehicles enter the road network passing through it), and the results compared. In Fig. 8., the traffic volumes (vehicles running in the system) per lane $\frac{N_R^{i,j}(t)}{a^{i,j}}$ are plotted on a time span from 08:00 to 16:00 h, for the cases of (a) normal conditions (b) ρ=1 hour disruption occurring at time 9:00 (i.e., rush time) in node 30 of road 2, (c) ρ=2 h disruption occurring at time 9:00 in node 30 of road 2, (d) ρ=1 hour disruption occurring at time 9:00 (i.e., rush time) in node 50 of road 3 (i.e., the one with the higher vehicle capacity and all vehicles pass through), and (e) ρ=2 h disruption occurring at time 9:00 in node 50 of road 3.

Table 3
ICVs and EVs parameters.

Parameters		Symbols	Values	References
EVs	EVs penetration level (%)	α	0, 25, 50, 75,100	
	Driving power of EVs (kW)	P_d	17.38	[46]
	Queuing for traffic power of EVs (kW)	P_q	6	[46]
	Charging power of EVs (kW)	P	75	[46]
	Critical SoC in vehicles (kWh)	$SoC_{critical}$	7	Minimum SoC to reach to the next CS
ICVs	Refilling rate of non-commercial ICVs (L/min)	q_v	32	[50]
	Refilling rate of commercial ICVs (L/min)	q_{v-c}	100	[51,52,53]
EVs and ICVs	Constant speed (mph)	U	65	[16]

It can be seen that nodes 43 to 62 (road 3) are critical, especially during rush hours when the $\frac{N_R^{i,j}(t)}{a^{i,j}}$ reaches values close to $c^{i,j} = 200$. This result would be exacerbated with the increase of α: in Figs. 9 and 10, the Probability Density Functions (PDFs) of the vehicles travel time for different levels of EVs penetration (α= 0 %, 25 %, 50 %, 75 % and 100 %) are plotted for incident in node 30 and node 50, respectively, showing the travel time increasing with the penetration level, due to the relevant contribution of charging and waiting for charging at the charging stations; Also, as expected, we can see that the severer the disruption ρ, the longer the travel time Tr. Disruption occurring in node 50, i.e., the critical node, cause more sever effects on the travel time in comparison with that occurring in node 30, meaning that the delay due to disruption could be relevant for the performance of the road power infrastructure.

The PDFs of the economic service losses due to the disruptions for each node can be calculated for different levels of α (Figs. 11 and 12): as α increases, the standard deviation of the $ESL_{EV_r \text{ or } ICV_p}(\Gamma, \rho)$ PDF increases, whereas as ρ increases, both mean and standard deviation of the $ESL_{EV_r \text{ or } ICV_p}(\Gamma, \rho)$ PDF increase (Figs. 13 and 14). Standard deviation of the $ESL_{EV_r \text{ or } ICV_p}(\Gamma, \rho)$ PDF for disruption in node 30 follows almost the same pattern for node 50 while the mean of the $ESL_{EV_r \text{ or } ICV_p}(\Gamma, \rho)$ PDF for disruption in node 30 is smaller than for node 50.

In Figs. 11 and 12, we can see that the $ESL_{EV_r \text{ or } ICV_p}(\Gamma, \rho)$ of the majority of the vehicles that are not jammed in the traffic is equal to zero; the negative values of $ESL_{EV_r \text{ or } ICV_p}(\Gamma, \rho)$ account for those vehicles that where jammed in the traffic congestion and have opted for a less congested and shorter path to reach the destination; the positive values of $ESL_{EV_r \text{ or } ICV_p}(\Gamma, \rho)$ account for those vehicles that were jammed in traffic congestion and have opted to change the route into less congested but longer paths. Let us assume, without loss of generality, an acceptable threshold delay of 15 % of the nominal coverage travel time, $\lambda = 0.15\Gamma$: Figs. 15 and 16 for disruption in node 30 and node 50, respectively, show the TR for $\rho = 1$ and $\rho = 2$; when α increases, TR reduces, i.e., as the number of EVs on the road network increases and the number of vehicles successfully completing their O-D travel within the desired time reduces, due to the EVs waiting for charging and, then, charging. Besides, TR of disruption in node 50 is lower than TR of disruption in node 30. This should alert the designers of integrated road-power network infrastructures where a hybrid fleet of EVs and ICVs is expected to run on: such negligible decrease in TR when ρ increases is only possible if energy supply by power grid is reliable, even in light of the demand increase due to EVs charging stations, the difficult coordination of EVs charging, and the challenging minimization of power losses and peak loads.

Beyond the quantitative results above presented, whose validity is limited to the case considered, the potential of the framework stands in enabling a straightforward comparison of the performance of the integrated road-power infrastructures under different disruption scenarios: simulations of disruptions of different duration and severity at specific nodes provide insights on how traffic flow is impacted, enabling informed decision-making regarding, for example, the optimal placement of gasoline and charging stations, the development of strategies for emergency management during disruptions, etc.. Without relying on such probabilistic framework of analysis, stakeholders may lack of uncertainty information to decide with confidence about planning to

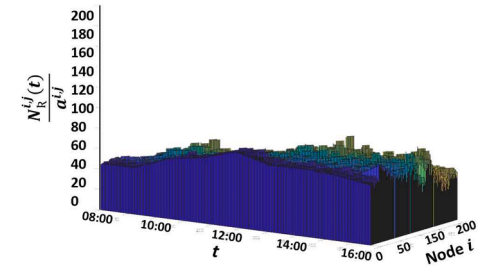

(a) normal condition

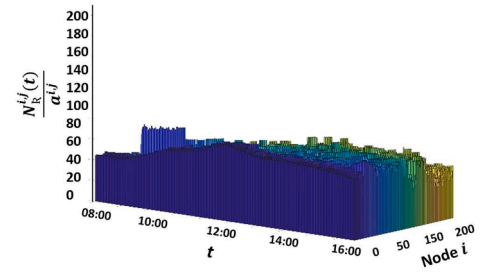

(b) 1 hour disruption ($\rho = 1h$) in node 30

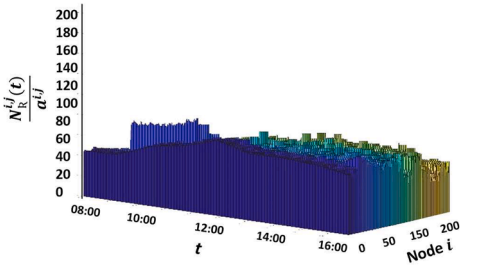

(c) 2 hours disruption ($\rho = 2h$) in node 30

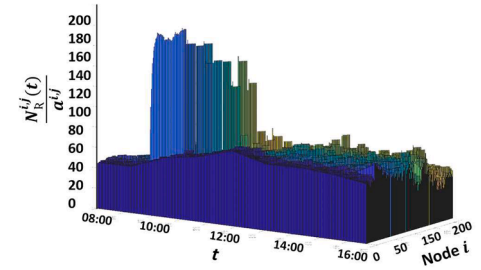

(d) 1 hour disruption ($\rho = 1h$) in node 50

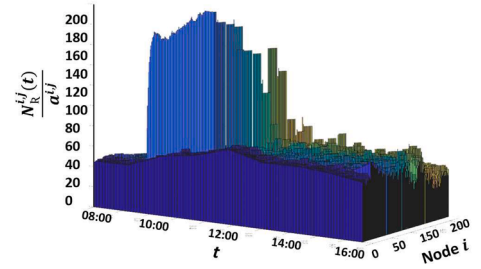

(e) 2 hours disruption ($\rho = 2h$) in node 50

Fig. 8. Traffic volume per lane, in each node of the transportation network from 8:00 to 16:00 for a) nominal conditions, b) 1 hour disruption ($\rho = 1h$) in node 30, c) 2 hours disruption ($\rho = 2h$) in node 30, b) 1 hour disruption ($\rho = 1h$) in node 50, c) 2 hours disruption ($\rho = 2h$) in node 50.

prepare for and respond to disruptions caused by events such as accidents (but also, to external events). Simulations enable simple comparisons of alternative solutions by identifying potential issues and searching for solutions.

The insights gained by the framework of analysis to inform decision making come with computational complexity that increases with the dimension of the integrated road-power infrastructure, the level of detail of the FMSs models adopted and the number of parameters therein. Table 4 shows the role played by the considered time horizon, disruption severity and EVs penetration level α on the computational time (in minutes): the longer the time horizon, the more the vehicles expected to run on the road and, therefore, the larger the number of FSMs simultaneously running and the associated computational time; the larger the severity, the more the vehicles queuing simultaneously and, thus, the larger the number of FSMs simultaneously running; the larger the penetration, the longer the computational time, because the EVs FSM is more burdensome than the FSM of ICVs. The computational burden is likely to increase when attempting to realistically modelling integrated road and power infrastructures, traffic flow of EVs and ICVs, power load under different scenarios of EVs penetration levels and various disruption scenarios.

5. Conclusion

In this paper, a probabilistic scenario analysis framework has been proposed to quantify the service losses related to delays that vehicles, both EVs and ICVs may incur due to different car accidental scenarios. The framework is based on modelling the SoS, comprised by road network, electric power system and vehicles, with graph theory and FSM (first research gap). FSM enables to assess the performance of a single vehicle, as well as of the integrated fleet of EVs and ICVs travelling on the road-power network, taking into account realistic (stochastic) characteristics like diversity of the EVs types, drivers charging attitudes and drivers road selection attitudes (second research gap). The proposed framework is powerful for modelling integrated systems of road and power infrastructures, traffic flow of EVs and ICVs, and dynamically assessing the distributed power load (third research gap), under different scenarios of EVs penetration levels and various disruption scenarios. In a realistic case study, two disruption scenarios with severity ρ of 1 hour and 2 hours have been considered, and the service losses, associated economic losses and transport reliability have been assessed. To address the last research gap, the service losses related to travel delays have been qualified as the ratio between the increase in travel time spent along the O-D routes due to a disruption and the corresponding expected time of travel in nominal conditions. The economic service losses have been computed as a function of the service losses, and thus ultimately associated with travel time. We extended the definition of TR as the probability that the economic service losses are less than an acceptable loss threshold. Based on the results of the case study, it can be concluded that EVs penetration might not affect the economic service losses and TR of the integrated road-power SoS, provided that the power system for EVs charging can adapt to the demand increase, by power coordination of EVs charging time, by control schemes and employing optimization methods to achieve systemic objectives like power loss minimization, peak load reduction, voltage regulation, distribution infrastructure overloading minimization, etc.

The proposed framework is shown to allow modelling the interconnections and interactions within the integrated road-power SoS, made of road network, power grid, EVs and ICVs. This allows enabling the identification of potential issues and the development of solutions to support EV growth, by quantifying a set of performance metrics under nominal conditions and disruption scenarios too. These metrics can help stakeholders make informed decisions about EV infrastructure choices and policies that can have significant long-term impacts on the environment, economy and society, in particular with respect to CO2 emission reduction. However, as also shown, the framework may result

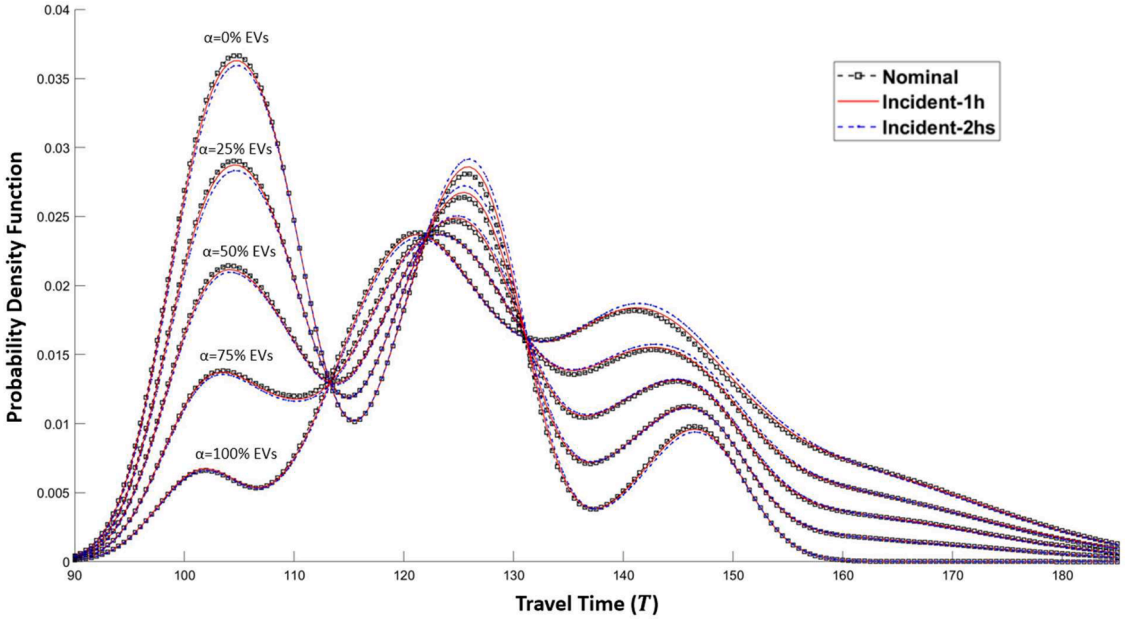

Fig. 9. PDF of vehicles (EVs + ICVs) travel time for an incident in node 30.

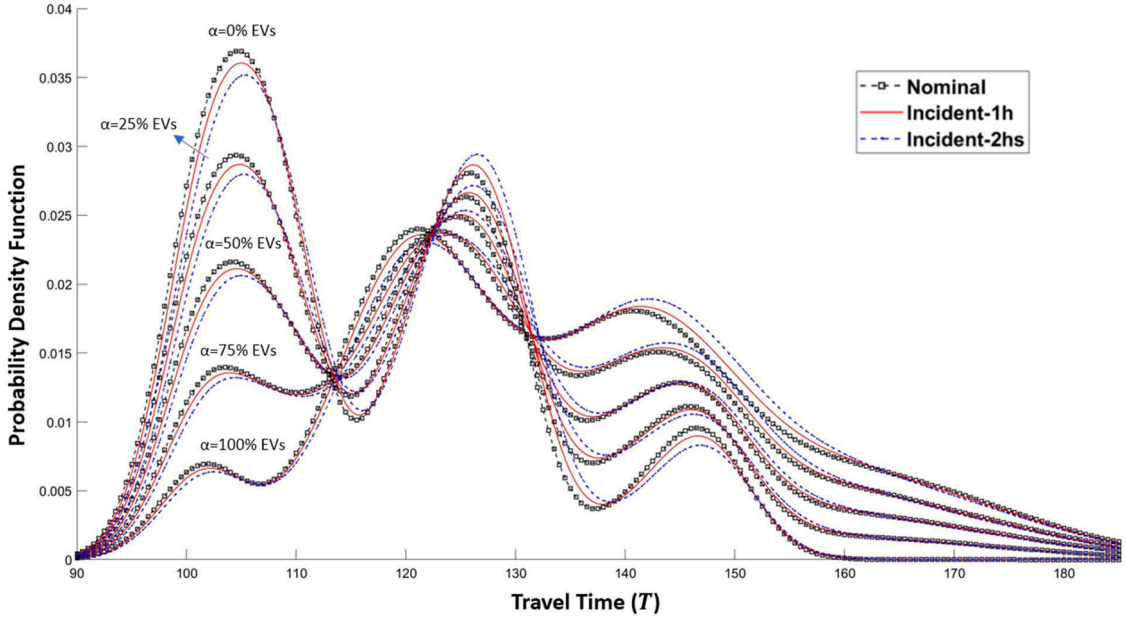

Fig. 10. PDF of vehicles (EVs + ICVs) travel time for an incident in node 50.

computationally burdensome when complex modelling and simulation are adopted with realistic assumptions, that challenge its scalability for the analysis of large systems. That said, several promising research directions can be pursued, including:

- Investigation of advanced simulation methods based on artificial intelligence and machine learning approaches to reduce the computational burden and, at the same time, increase the realism in the modelling assumptions, amongst which we can list:
  - the dimension of the road and power infrastructure that may reach hundreds thousands of road intersections and dispatchment nodes, respectively;
  - the EVs charging attitude and coordination amongst different charging stations, which influence the performance of the integrated road-power network in terms of peak load, voltage regulation and power losses;
  - the actual role of EVs on the reduction of greenhouse gas emissions, improvement of air quality and public wellbeing;
- Exploring the use of advanced optimization methods to optimally design the integrated road-power infrastructure so as to pursue the minimization of vehicles travel time and voltage instability under a large spectrum of possible disruption scenarios.
- Conducting a rigorous and structured sensitivity analysis to determine the impact on the optimization results of different parameters,

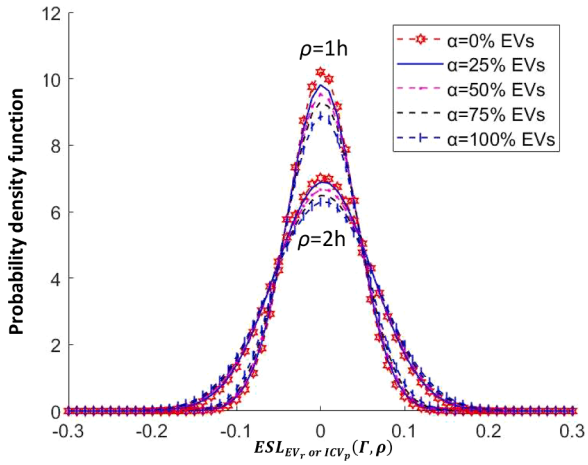

Fig. 11. PDF of the economic service losses due to the disruptions in node 30.

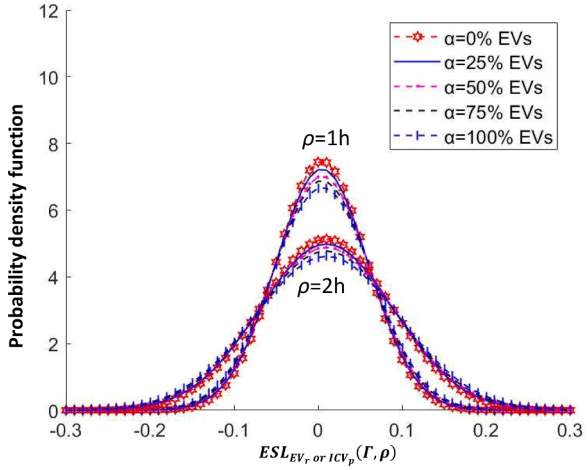

Fig. 12. PDF of the economic service losses due to the disruptions in node 50.

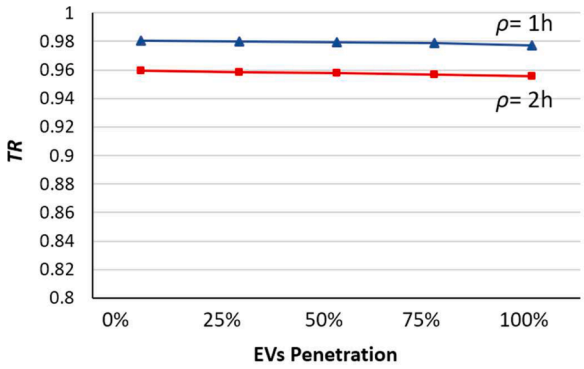

Fig. 15. Transport Reliability for disruptions in node 30.

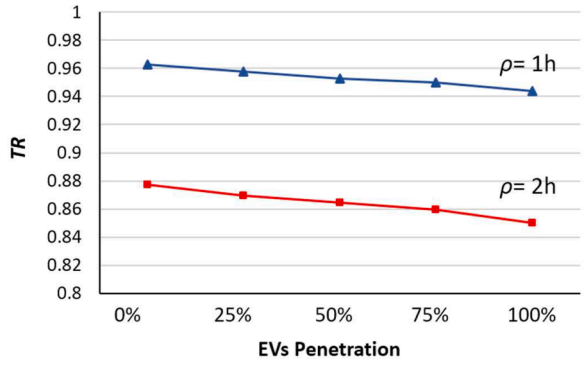

Fig. 16. Transport Reliability for disruptions in node 50.

such as EVs penetration rate, travel demand, and charging infrastructure capacity, to inform the decision makers on the most sensitive information for decision-making regarding, for example, the optimal placement of gas and charging stations, as the development of strategies for emergency management during disruptions.

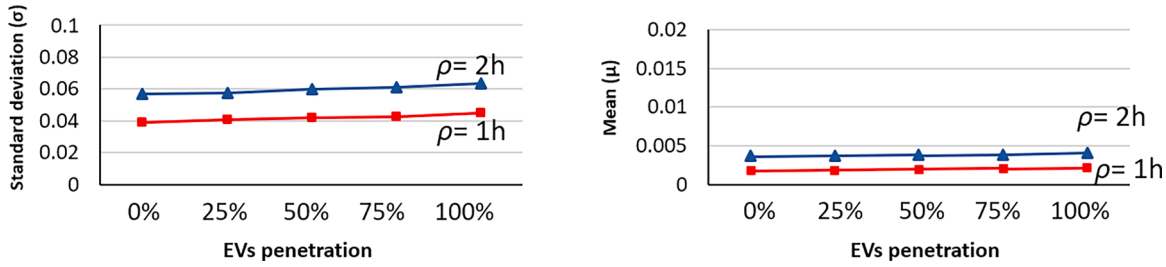

Fig. 13. Standard deviation and mean of the PDF $ESL_{EV_r\ or\ ICV_p}(\Gamma,\rho)$ for disruptions in node 30.

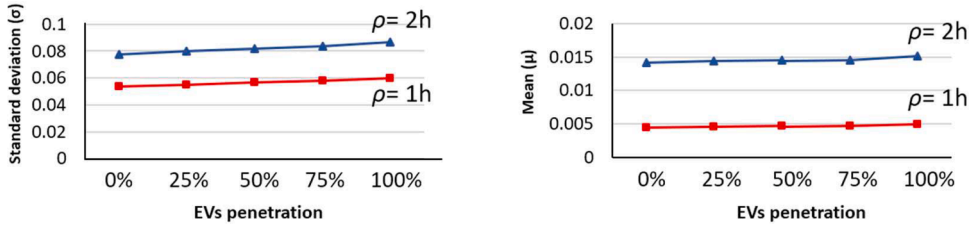

Fig. 14. Standard deviation and mean of the PDF $ESL_{EV_r\ or\ ICV_p}(\Gamma,\rho)$ for disruptions in node 50.

Table 4
Computational time.

Time horizon	Disruption severity	Computational time (min)				
		α = 0%	α = 25%	α = 50%	α = 75%	α = 100%
00:00 to 24:00	ρ=0	126	171	223	292	380
08:00 to 16:00	ρ=0	32	34	40	48	54
	ρ=1	43	46	54	62	69
	ρ=2	58	63	69	76	85

CRediT authorship contribution statement

Lida Naseh Moghanlou: Conceptualization, Data curation, Software, Formal analysis, Writing – original draft, Investigation. **Francesco Di Maio:** Conceptualization, Data curation, Formal analysis, Writing – original draft. **Enrico Zio:** Conceptualization, Data curation, Validation, Formal analysis, Writing – original draft.

Declaration of Competing Interest

The authors declare the following financial interests/personal relationships which may be considered as potential competing interests:

Lida Naseh Moghanlou reports financial support was provided by MUR, Energy for Motion Project, Dipartimenti Eccellenti 2018–2022.

Data availability

Data will be made available on request.

Acknowledgement

Lida Naseh Moghanlou acknowledges the financial support from the Energy for Motion Project "Dipartimenti Eccellenti 2018–2022", funded by MUR.

Appendix A

FSM for Modelling EVs or ICVs

For modelling EV or ICV motion, a FSM with six states $S = \{S_0, S_1, S_2, S_3, S_4, S_5\}$ (Fig. 3) is elaborated from the one presented in [20]. Besides the initial "start-up" state S_0 and "shut-down" state S_3, we consider a "driving" state S_1 and a "queuing for traffic" state S_2, a "charging" or "refilling" state S_4 and a "queuing for charging" or "queuing for refilling" state S_5. In general terms, the generic r-th EV, EV_r, or p-th ICV, ICV_p, starts the trip with an entrance SoC, $SoC_r(t_{r,in})$, or Fuel Level (FL), $FL_p(t_{p,in})$, at its entrance time $t_{r,in}$ or $t_{p,in}$, and is found at time t in edge i,j ($i \neq j$) with state S_m according to the transition rule $f(S_m,\ i,\ \bar{\theta})$, which dependents on

$$\bar{\theta} = \left\{N_{\mathrm{R}}^{i+1,j+1}(t),\ SoC_r(t)\ or\ FL_p(t),\ N_{CS_x}(t)\ or\ N_{GS_\xi}(t)\right\}$$

, where

$$N_R^{i+1,j+1}(t)$$

is the number of vehicles occupying the edge $i+1.j+1$ of road

$$R$$

at time t, $SoC_r(t)$ or $FL_p(t)$ is the SoC or FL of EV_r *or* ICV_p at time t, and $N_{CS_x}(t)$ *or* $N_{GS_\xi}(t)$ is the number of the EVs or ICVs which are charging or refilling in the x-th or ξ-th charging station CS_x or gas station GS_ξ at time t. In practical words, we model the mobility dynamics such that when a generic EV_r *or* ICV_p of the pool of N_{EVs} EVs *or* N_{ICVs} ICVs starts a trip, it switches from state S_0 to state S_1 if the number of vehicles occupying the next edge at time t,

$$N_R^{i+1,j+1}(t)$$

, is smaller than the edge maximum capacity of vehicles $c^{i+1,j+1}$; whereas it switches from S_0 to S_2, if

$$N_R^{i+1,j+1}(t)$$

is equal to $c^{i+1,j+1}$, i.e., the edge has reached its maximum capacity and cannot accommodate other vehicles. As EV_r *or* ICV_p moves forward on edge i,j where the charging station CS_x or gas station GS_ξ is located, if $SoC_r(t)$ or $FL_p(t)$ is at the lowest critical amount, $SoC_{critical}$ for EVs or $FL_{critical}$ for non-commercial ICVs or $SoC_{critical}$ for *EVs* or $FL_{critical}$ for non − commercial ICVs or $FL_{critical-c}$ for commercial ICVs, it may switch to state S_4 in order to recharge or refill, unless the number of EVs charging in CS_x, $N_{CS_x}(t)$ or number of ICVs refilling in GS_ξ, $N_{GS_\xi}(t)$ at time t is equal to the maximum capacity of vehicles for that charging station, $C_{CS_x}^{max}$ or gas station, $C_{GS_\xi}^{max}$: in this case, EV_r *or* ICV_p switches to state S_5 and later switches to state S_4 to recharge or refill when $N_{CS_x}(t) < C_{CS_x}^{max}$ or $N_{GS_\xi}(t) < C_{GS_\xi}^{max}$. Bedsides taking into account the diversity of EVs battery type B_r, we consider the driver charging attitude, $ch_r(t)$, which describes the fact that each EV driver has a specific preference value of SoC at which to recharge. We also take into account the diversity of ICVs size and their tank capacities for non-commercials and commercials, $Tank_p$ and $Tank_{p-c}$, respectively, which means that a specific FL (equal to $Tank_p$ *or* $Tank_{p-c}$) for each ICV is required to be refilled at the gas stations. Upon charging or refilling completion, EV_r *or* ICV_p switches to state S_1 and continues the trip switching amongst its states according to the transition rules $f(S_m,\ i,\ \bar{\theta})$, finally reaching the destination node at which time it switches to state S_3. In synthesis, the states transition rules for the r-th EV at time t, are formulated as:

$$f(S_m, i, \bar{\theta}) = \begin{cases} S_{m+1} = S_1 \ \ if \ \ N_{\mathrm{R}}^{i+1,j+1}(t) < c^{i+1,j+1} \\ S_{m+1} = S_2 \ \ if \ \ N_{\mathrm{R}}^{i+1,j+1}(t) = c^{i+1,j+1} \\ S_{m+1} = S_4 \ \ if \ \ SoC_r(\mathrm{t}) \leq SoC_{critical} \ \ and \ \ N_{CS_x}(\mathrm{t}) < C_{CS_x}^{max} \\ S_{m+1} = S_5 \ \ if \ \ SoC_r(\mathrm{t}) \leq SoC_{critical} \ \ and \ \ N_{CS_x}(\mathrm{t}) = C_{CS_x}^{max} \end{cases} \quad (A.1)$$

Also, for each EV_r, the SoC can be evaluated in time as described in Equation (A.2), in dependence of the S_m sequence from start-up state S_0 to shut-down state S_3.

$$SoC_r(t) = \begin{cases} SoC_r(t-T) - P_d.T \;\; S = S_1 \\ SoC_r(t-T) - P_q.T \;\; S = S_2 \\ SoC_r(t-T) + P.T \;\; S = S_4 \\ SoC_r(t-T) \;\; S = S_5 \end{cases} \tag{A.2}$$

where P_d is the power absorbed during driving, P_q is that during queuing for traffic, P is the charging power and T is the travel time interval.

In conclusion, the state transition rules for the generic p-th ICV at time t, are formulated as follows:

$$f(S_m, i, \bar{\theta}) = \begin{cases} S_{m+1} = S_1 \;\; if \;\; N_{\mathrm{R}}^{i+1,j+1}(t) < c^{i+1,j+1} \\ S_{m+1} = S_2 \;\; if \;\; N_{\mathrm{R}}^{i+1,j+1}(t) = c^{i+1,j+1} \\ S_{m+1} = S_4 \;\; if \;\; FL_p(\mathrm{t}) \le FL_{critical} \text{ or } FL_p(\mathrm{t}) \le FL_{critical-c} \;\; and \;\; N_{GS_\xi}(\mathrm{t}) < C_{GS_\xi}^{max} \\ S_{m+1} = S_5 \;\; if \;\; FL_p(\mathrm{t}) \le FL_{critical} \text{ or } FL_p(\mathrm{t}) \le FL_{critical-c} \;\; and \;\; N_{GS_\xi}(\mathrm{t}) = C_{GS_\xi}^{max} \end{cases} \tag{A.3}$$

For each ICV_p, the FL is evaluated as described in Equation (A.4) below, in dependence on the S_m sequence of the ICV_p from start-up S_0 to shut-down S_3:

$$FL_p(t) = \begin{cases} FL_p(t-T) - F_p^{dr} \; or \; FL_p(t-T) - F_{p-c}^{dr} \;\; S = S_1 \\ FL_p(t-T) - F_p^{id} \; or \; FL_p(t-T) - F_{p-c}^{id} \;\; S = S_2 \\ FL_p(t-T) + q_v.T \; or \; FL_p(t-T) + q_{v-c}.T \;\; S = S_4 \\ FL_p(t-T) \;\; S = S_5 \end{cases} \tag{A.4}$$

where F_p^{dr} and F_{p-c}^{dr} are the fuel consumption rates of non-commercial and commercial ICVs during driving, respectively, F_p^{id} and F_{p-c}^{id} are the fuel consumption rates for traffic of non-commercial and commercial ICVs during queuing, respectively, q_v and q_{v-c} are the refilling rates of non-commercial and commercial ICVs, respectively, and T is considered the travel time interval.

References

[1] Wang H, Fang YP, Zio E. Resilience-oriented optimal post-disruption reconfiguration for coupled traffic-power systems. Reliab Eng Syst Saf 2022;222:108408. 2022.

[2] Arango E, Nogal M, Yang M, Sousa HS, Stewart MG, Matos JC. Dynamic thresholds for the resilience assessment of road traffic networks to wildfires. Reliab Eng Syst Saf 2023:109407.

[3] Sharma N, Gardoni P. Mathematical modeling of interdependent infrastructure: an object-oriented approach for generalized network-system analysis. Reliab Eng Syst Saf 2022;217:108042.

[4] Liu X, Fang YP, Zio E. A hierarchical resilience enhancement framework for interdependent critical infrastructures. Reliab Eng Syst Saf 2021;215:107868.

[5] Kong J, Zhang C, Simonovic SP. Optimizing the resilience of interdependent infrastructures to regional natural hazards with combined improvement measures. Reliab Eng Syst Saf 2021;210:107538.

[6] Sun L, d'Ayala D, Fayjaloun R, Gehl P. Agent-based model on resilience-oriented rapid responses of road networks under seismic hazard. Reliab Eng Syst Saf 2021;216:108030.

[7] Zio E, Ferrario E. A framework for the system-of-systems analysis of the risk for a safety-critical plant exposed to external events. Reliab Eng Syst Saf 2013;114:114–25.

[8] Zio E. Reliability analysis of systems of systems. IEEE Reliab. Mag. 2016:1–6. Feb. 2016(Spec. Iss.).

[9] Mo HD, Li YF, Zio E. A system-of-systems framework for the reliability analysis of distributed generation systems accounting for the impact of degraded communication networks. Appl. Energy 2016;183:805–22.

[10] Gu Y, Fu X, Liu Z, Xu X, Chen A. Performance of transportation network under perturbations: reliability, vulnerability, and resilience. Transp Res Part E: Logist Transp Rev 2020;133:101809.

[11] Edrissi A, Nourinejad M, Roorda MJ. Transportation network reliability in emergency response. Transp Res Part E: Logist Transp Rev 2015;80:56–73.

[12] Kurth M, Kozlowski W, Ganin A, Mersky A, Leung B, Dykes J, Kitsak M, Linkov I. Lack of resilience in transportation networks: economic implications. Transp Res Part D Transp Environ 2020;86:102419.

[13] Wei W, Danman WU, Qiuwei WU, Shafie-Khah M, Catalao JP. Interdependence between transportation system and power distribution system: a comprehensive review on models and applications. J Modern Power Syst Clean Energy 2019;7(3):433–48.

[14] Gandoman FH, Ahmadi A, Van den Bossche P, Van Mierlo J, Omar N, Nezhad AE, Mavalizadeh H, Mayet C. Status and future perspectives of reliability assessment for electric vehicles. Reliab Eng Syst Saf 2019;183:1–16.

[15] Tang D, Wang P. Nodal impact assessment and alleviation of moving electric vehicle loads: from traffic flow to power flow. IEEE Trans Power Syst 2016;31(6):4231–42.

[16] Wang H, Fang YP, Zio E. Risk assessment of an electrical power system considering the influence of traffic congestion on a hypothetical scenario of electrified transportation system in New York state. IEEE Trans Intell Transp Syst 2019.

[17] Ouyang M. Review on modeling and simulation of interdependent critical infrastructure systems. Reliab Eng Syst Saf 2014;121:43–60.

[18] Suo W, Wang L, Li J. Probabilistic risk assessment for interdependent critical infrastructures: a scenario-driven dynamic stochastic model. Reliab Eng Syst Saf 2021;214:107730.

[19] Zhou J, Huang N, Coit DW, Felder FA. Combined effects of load dynamics and dependence clusters on cascading failures in network systems. Reliab Eng Syst Saf 2018;170:116–26.

[20] Naseh Moghanlou L, Hoseyni SM, Di Maio F, Zio E. Finite state machine modelling for the performance analysis of an integrated road-power infrastructure with a hybrid fleet of EVs and ICVs. In: Proceedings of the 31st European Safety and Reliability Conference; 2021.

[21] Hong L, Ouyang M, Peeta S, He X, Yan Y. Vulnerability assessment and mitigation for the Chinese railway system under floods. Reliab Eng Syst Saf 2015;137:58–68.

[22] Shafieezadeh A, Burden LI. Scenario-based resilience assessment framework for critical infrastructure systems: case study for seismic resilience of seaports. Reliab Eng Syst Saf 2014;132:207–19.

[23] Ahmadzai F, Rao KL, Ulfat S. Assessment and modelling of urban road networks using Integrated Graph of Natural Road Network (a GIS-based approach. J Urban Manag 2019;8(1):109–25.

[24] Anderson S, Nair V. Electric vehicle charge scheduling on highway networks from an aggregate cost perspective. 2018.arXiv preprint arXiv:1901.03017.

[25] Storm PJ, Mandjes M, Arem BV. Efficient evaluation of stochastic traffic flow models using Gaussian process approximation. Transp Res Part B Methodol 2022;164:126–44.

[26] Rocchetta R, Li Y, Zio E. Risk assessment and risk-cost optimization of distributed power generation systems considering extreme weather conditions. Reliab Eng Syst Saf 2015;136:47–61.

[27] Yuan Z, Feng-Chun S, Hong-wen H. Global Control Simulation of Electric Vehicle Based on Finite State Machine Theory. J Beijing Inst Technol 2004;(S1):68–72.

[28] Mu Y, Wu J, Jenkins N, Jia H, Wang C. A spatial–temporal model for grid impact analysis of plug-in electric vehicles. Appl Energy 2014;114:456–65.

[29] Hou K, Xu X, Jia H, Yu X, Jiang T, Zhang K, Shu B. A reliability assessment approach for integrated transportation and electrical power systems incorporating electric vehicles. IEEE Trans Smart Grid 2016;9(1):88–100.

[30] Wang J, Peeta S, He X. Multiclass traffic assignment model for mixed traffic flow of human-driven vehicles and connected and autonomous vehicles. Transp Res Part B Methodol 2019;126:139–68.

[31] Sun C, Pei X, Hao J, Wang Y, Zhang Z, Wong SC. Role of road network features in the evaluation of incident impacts on urban traffic mobility. Transp Res Part B Methodol 2018;117:101–16.

[32] Bae S, Kwasinski A. Spatial and temporal model of electric vehicle charging demand. IEEE Trans Smart Grid 2011;3(1):394–403.

[33] Chen R, Qian X, Miao L, Ukkusuri SV. Optimal charging facility location and capacity for electric vehicles considering route choice and charging time equilibrium. Comput Oper Res 2020;113:104776.
[34] Wang X, Shahidehpour M, Jiang C, Li Z. Coordinated planning strategy for electric vehicle charging stations and coupled traffic-electric networks. IEEE Trans Power Syst 2018;34(1):268–79.
[35] He F, Yin Y, Lawphongpanich S. Network equilibrium models with battery electric vehicles. Transp Res Part B Methodoll 2014;67:306–19.
[36] Xie C, Jiang N. Relay requirement and traffic assignment of electric vehicles. Comput Aid Civ Infrast Eng 2016;31(8):580–98.
[37] Wang X, Shahidehpour M, Jiang C, Li Z. Resilience enhancement strategies for power distribution network coupled with urban transportation system. IEEE Trans Smart Grid 2018;10(4):4068–79.
[38] Ganin AA, Kitsak M, Marchese D, Keisler JM, Seager T, Linkov I. Resilience and efficiency in transportation networks. Sci Adv 2017;3(12):e1701079.
[39] Ziogou C, Krinidis S, Ioannidis D, Papadopoulou S, Tzovaras D, Voutetakis S. An intelligent decision making and notification system based on a knowledge-enabled supervisory monitoring platform. Comput Aid Cheml Eng 2016;38:1353–8.
[40] Monteir JC, Arlindo LO. Finite state machine decomposition for low power. In: Proceedings of the 35th annual Design Automation Conference; 1988. p. 758–63.
[41] Hejase M, Kurt A, Aldemir T, Ozguner U, Guarro S, Yau MK, Knudson M. A quantitative and risk based framework for uas control system assurance. AIAA Information Systems-AIAA Infotech@ Aerospace; 2017. p. 0882.
[42] Zhang M, Li N, Girard A, Kolmanovsky I. A finite state machine based automated driving controller and its stochastic optimization. Virginia: American Society of Mechanical Engineers; 2017.
[43] TranSight 4.2 user guide. Regional Economic Models Inc., Amherst, MA; 2018.
[44] New York state department of transportation website, 2007. [Online]. Available at: gis3.dot.ny.gov/tdvpdf/YR2007/Other/Class/R07/71_Clinton/71_0055_ClassAverageReport.pdf [Accessed: Feb. 21, 2018].
[45] New York state department of transportation website, 2015. [Online]. Available: gis3.dot.ny.gov/tdvpdf/YR2015/Other/Class/R07/71_Clinton/71_0224_2015_ClassAverageReport.pdf [Accessed: Feb. 21, 2018].
[46] [*Online*]. Available: www.car-specs.net/ev-database.org [Accessed: March 2020].
[47] Su W, Rahimi Eichi H, Zeng W, Chow MY. A Survey on the Electrification of Transportation in a Smart Grid Environment. IEEE Trans Ind Inf 2012;8(1):1–10. Volume vol.
[48] Wang H, Abdin AF, Fang YP, Zio E. Resilience assessment of electrified road networks subject to charging station failures. Comput Aided Civ Infrastruct Eng 2021.
[49] [*Online*]. Available: dmv.ny.gov/statistic/2017reginforce-web.pdf [Accessed: Nov. 27, 2019].
[50] [*Online*]. Available: https://www.carandbike.com.
[51] [*Online*]. Available: www.energy.gov/eere/vehicles/fact-625-may-31-2010-distribution-trucks-road-vehicle-weight.
[52] [*Online*]. Available: www.merchantsfleet.com/industry-insights/best-cargo-vans-for-business/.
[53] Garg M, Sharpe B. Fuel consumption standards for heavy-duty vehicles in India. ICCT report; 2017.